Research Paper

Anthocyanins protect the gastrointestinal tract from high fat diet-induced alterations in redox signaling, barrier integrity and dysbiosis

Eleonora Cremonini[a,b], Elena Daveri[a,b], Angela Mastaloudis[c], Ana M. Adamo[d,e], David Mills[f,g], Karen Kalanetra[f,g], Shelly N. Hester[c], Steve M. Wood[c], Cesar G. Fraga[a,h,i], Patricia I. Oteiza[a,b,*]

[a] Departments of Nutrition, University of California, Davis, CA, USA
[b] Environmental Toxicology, University of California, Davis, CA, USA
[c] Pharmanex Research, NSE Products, Inc., Provo, UT, USA
[d] Quimica Biológica Patológica, Facultad de Farmacia y Bioquímica, Universidad de Buenos Aires, Buenos Aires, Argentina
[e] Instituto de Química y Fisicoquímica Biológicas (IQUIFYB), CONICET-Universidad de Buenos Aires, Buenos Aires, Argentina
[f] Food Science and Technology, University of California, Davis, CA, USA
[g] Viticulture and Enology, University of California, Davis, CA, USA
[h] Fisicoquímica, Facultad de Farmacia y Bioquímica, Universidad de Buenos Aires, Buenos Aires, Argentina
[i] Instituto de Bioquímica y Medicina Molecular (IBIMOL), CONICET-Universidad de Buenos Aires, Buenos Aires, Argentina

ABSTRACT

The gastrointestinal (GI) tract can play a critical role in the development of pathologies associated with overeating, overweight and obesity. We previously observed that supplementation with anthocyanins (AC) (particularly glycosides of cyanidin and delphinidin) mitigated high fat diet (HFD)-induced development of obesity, dyslipidemia, insulin resistance and steatosis in C57BL/6J mice. This paper investigated whether these beneficial effects could be related to AC capacity to sustain intestinal monolayer integrity, prevent endotoxemia, and HFD-associated dysbiosis. The involvement of redox-related mechanisms were further investigated in Caco-2 cell monolayers. Consumption of a HFD for 14 weeks caused intestinal permeabilization and endotoxemia, which were associated with a decreased ileum expression of tight junction (TJ) proteins (occludin, ZO-1 and claudin-1), increased expression of NADPH oxidase (NOX1 and NOX4) and NOS2 and oxidative stress, and activation of redox sensitive signals (NF-κB and ERK1/2) that regulate TJ dynamics. AC supplementation mitigated all these events and increased GLP-2 levels, the intestinal hormone that upregulates TJ protein expression. AC also prevented, *in vitro*, tumor necrosis factor alpha-induced Caco-2 monolayer permeabilization, NOX1/4 upregulation, oxidative stress, and NF-κB and ERK activation. HFD-induced obesity in mice caused dysbiosis and affected the levels and secretion of MUC2, a mucin that participates in intestinal cell barrier protection and immune response. AC supplementation restored microbiota composition and MUC2 levels and distribution in HFD-fed mice. Thus, AC, particularly delphinidin and cyanidin, can preserve GI physiology in HFD-induced obesity in part through redox-regulated mechanisms. This can in part explain AC capacity to mitigate pathologies, i.e. insulin resistance and steatosis, associated with HFD-associated obesity.

1. Introduction

The gastrointestinal (GI) tract plays a major role in sustaining human health and alterations in GI tract physiology are associated with systemic effects that can contribute to the development of various pathologies [1]. Malnutrition, e.g. high fat diets, overweight, and obesity, affect intestinal function and are known to contribute to the development of insulin resistance, type 2 diabetes (T2D), and non-alcoholic fatty liver disease (NAFLD), among other pathological conditions [2–6].

Intestinal health is in part determined by a functional intestinal barrier, an appropriate microbiota, and controlled levels of

inflammation. These three components of intestinal physiology are interrelated: i) intestinal permeabilization can lead to the paracellular transport of endotoxins present in food or those generated by the luminal microbiota, which once in the circulation, can trigger systemic inflammatory responses [5,7,8]; ii) modifications in microbiota composition can affect intestinal barrier function, endotoxin production, and the synthesis of trophic and energy-regulating hormones [9–12]; and iii) in a mutualistic relationship, the immune system and the microbiota interact to sustain intestinal health [13,14]. Given the role of the gastrointestinal tract on energy homeostasis, restoration and/or conservation of integrity of the intestinal barrier and microbial balance may be effective strategies for optimizing metabolism, and prevent the development of metabolic dysregulation and associated pathologies.

Dietary bioactives can have a major influence on GI tract function, and subsequently, on its impact on overall health. Select flavonoids have multiple actions at the level of the GI tract that could explain the systemic effects associated with their consumption [10,15]. Several health benefits have been attributed to the flavonoid subfamily of anthocyanins (AC). With regard to the GI tract, we previously observed that AC protected *in vitro* Caco-2 intestinal cell monolayers from tumor necrosis alpha (TNFα)-induced permeabilization [16]. This effect was dependent on AC structure, cyanidin and delphinidin being the most effective. A subsequent *in vivo* study showed that supplementing the diet with a berry extract rich in both cyanidin and delphinidin mitigated high fat diet (HFD)-induced development of obesity, dyslipidemia, insulin resistance and steatosis in C57BL/6J mice [17]. We observed that AC modulated cell redox conditions, decreasing the expression of select NADPH oxidases and attenuating oxidative stress and redox-regulated signaling pathways, e.g. NF-κB and mitogen activated protein kinases (MAPKs).

This paper investigated whether the previously reported beneficial effects of supplementation with cyanidin and delphinidin mitigating insulin sensitivity and steatosis in HFD-fed C57BL/6J mice [17] could be in part due to their protective actions on intestinal monolayer integrity, endotoxemia, and modulation of the associated dysbiosis. The involved mechanisms were further investigated *in vitro* in Caco-2 cell monolayers. Cyanidin and delphinidin protected the monolayer integrity by preventing the loss of tight junction (TJ) structure and function. These effects seem to occur in part via the modulation of NADPH oxidase expression, prevention of oxidative stress, and downstream, inhibition of NF-κB, and of the MAPK ERK1/2 pathways. Simultaneously, AC acted by stimulating the production of the GI trophic hormone GLP-2 and restoring the normal composition of the microbiota.

2. Materials and methods

2.1. Materials

Caco-2 cells were from the American Type Culture Collection (Rockville, MA). Cell culture media and reagents were from Invitrogen/Life Technologies (Grand Island, NY). HBSS 1X (21-022-CV) was obtained from Corning (Manassas, VA). The Millicell cell culture inserts were from EMD Millipore (Hayward, CA). Human interferon gamma (IFN-γ) and primary antibodies for β-actin (#12620), phosphor (Ser536) p65 (#3033), p65 (3987), phosphor (Thr202/Tyr204) ERK1/2 (#4370), ERK1/2 (#9102), and phosphor (Thr18/Ser19) MLC (#3671) were from Cell Signaling Technology (Danvers, MA). Antibodies for HSC-70 (SC-1059), and nitric oxide synthase 2 (NOS2) (sc-649) were from Santa Cruz Biotechnology (Santa Cruz, CA, USA). Antibodies for ZO-1 (33–9100), occludin (71–1500), and claudin-1 (71–7800) were from Invitrogen (Carlsbad, CA). Antibodies for 4-hydroxynonenal (4-HNE) (ab46545), NOX4 (ab216654) and NOX1 (ab55831) were from Abcam Inc. (Cambridge, MA). PVDF membranes were obtained from BIO-RAD (Hercules, CA, USA). The Enhanced chemiluminescence (ECL) Western blotting system was from Thermo Fisher Scientific Inc.

(Piscataway, NJ). Fluorescein isothiocyanate (FITC)-dextran (4 kDa), protocatechuic acid (PCA), and all other chemicals were purchased from Sigma-Aldrich Co (St. Louis, MO). Endotoxin levels were determined using a kit from Lonza (Basel, Switzerland). GLP-2 was determined using a kit from Crystal Chem Inc (Downers Grove, IL). The AC-rich mix was provided by NSE Products, Inc. (Provo, UT) and its composition is described in Ref. [17]. Delphinidin-3-O-glucoside, cyanidin-3-O-glucoside, and peonidin-3-O-glucoside were from Extrasynthese (Genay Cedex, France).

2.2. Animals and animal care

All procedures were in agreement with standards for care of laboratory animals as outlined in the NIH Guide for the Care and Use of Laboratory Animals; experimental protocols were approved before implementation by the University of California, Davis Animal Use and Care Administrative Advisory Committee. Procedures were administered under the auspices of the Animal Resource Services of the University of California, Davis.

Healthy male C57BL/6J mice (20–25 g) (10 mice/group) were fed for 14 w either: i) a diet containing approximately 10% total calories from fat (Control, C group); ii) the control diet plus 40 mg AC/kg body weight (CA group); iii) a diet containing approximately 60% total calories from fat (lard) (HF group); or iv) the high fat diet supplemented with 40 mg AC/kg body weight (HFA40 group). Considering the dose translation from animals to humans [18], the amount of AC consumed by mice in the current study corresponds to a human equivalent intake of 225 mg of AC per day. Although average daily consumption of AC is lower in human populations, a cup of berries would provide similar amounts (e.g. 240 and 175 mg AC per 100 g of raw blueberries and blackcurrants, respectively).

After 14 weeks on the dietary treatments, mice were euthanized by cervical dislocation. Blood from the submandibular vein was collected into heparinized tubes, and plasma isolated after centrifugation at $3,000 \times g$ for 10 min at room temperature. The intestine was dissected, measured, divided into its different portions (duodenum, jejunum, ileum and colon). Tissues were rinsed with PBS containing protease inhibitors, flash frozen in liquid nitrogen, and then stored at $-80\,°C$ until further analysis. The overall metabolic profile of these animals has been recently published [17]. Plasma GLP-2 and endotoxin concentrations were determined following the manufacturer's protocols.

2.3. Intestinal permeability

Intestinal permeability was measured after 8 weeks on the diets as described previously [10]. Mice were fasted for 4 h then gavaged with FITC-dextran 4 kDa (200 mg/kg body weight). After 90 min, 100 μl of blood was collected from the tip of the tail vein. The blood was kept in the dark and centrifuged at $3,000 \times g$ for 10 min at room temperature, and the serum collected. Serum aliquots (20 μl) and a standard curve of FITC-dextran were plated in 96-well plates and diluted to 200 μl with 0.9% (w/v) NaCl. Fluorescence was measured using a microplate spectrofluorometer (Synergy H1, BioTek, Winooski, USA) at λexc: 495 nm and λem: 520 nm.

2.4. Cell culture and incubations

Caco-2 cells were cultured at 37 °C and 5% (v/v) CO$_2$ atmosphere in minimum essential medium (MEM) supplemented with 10% (v/v) fetal bovine serum, antibiotics (50 U/ml penicillin, and 50 μg/ml streptomycin), 1% (v/v) of 100X non-essential amino acids, and 1 mM sodium pyruvate. The medium was replaced every 3 d during cell growth and differentiation. For the experiments, cells were used 18 d after reaching confluence to allow for differentiation into intestinal epithelial cells. Cells were used between passages 3 and 15. All the experiments were performed in serum- and phenol red-free MEM.

2.5. Evaluation of Caco-2 monolayer permeability

Caco-2 monolayer permeability was evaluated by measuring the transepithelial electrical resistance (TEER) and the paracellular transport of FITC-dextran as previously described [16]. For both methods, cells were differentiated into polarized monolayers. For the evaluation of TEER and FITC-dextran permeability, Caco-2 cell monolayers were preincubated for 24 h with IFNγ (10 ng/ml) to upregulate the TNFα receptor [19]. The monolayers were then incubated for 30 min with the AC mix, protocatechuic acid (PCA), or the 3-O-glucosides of cyanidin, delphinidin or peonidin added to the upper compartment. To promote monolayer permeabilization, monolayers were treated with TNFα (5 ng/ml) added to the lower chamber. Cells were incubated for 6 h further for TEER evaluation or 9.5 h for FITC-dextran permeability determination. TEER was measured using a Millicell-ERS Resistance System (Millipore, Bedford, MA) that includes a dual electrode volt-ohm-meter. TEER was calculated as: TEER = $(R_m - R_i)$ x A(R_m, transmembrane resistance; R_i, intrinsic resistance of a cell-free media; and A, the surface area of the membrane in cm^2). The apical-to-basolateral clearance (CL) of FITC-dextran (4 kDa) was calculated using the equation $f_{FITC}/(F_{FITC}/A)$, where f_{FITC} is the flux of FITC-dextran (in fluorescence units/h); F_{FITC}, the fluorescence of FITC-dextran in the upper compartment at zero time (in fluorescence units per nl); and A, the surface area of the membrane (1 cm^2). Arbitrary units (AU) were calculated based on TEER or CL values for the non-added (control) cells.

2.6. Western blot analysis

Homogenates were prepared in lysis buffer containing 4x amount of protease inhibitors using a bead tissue homogenizer (Bead Mill 24, Fisher Scientific, Waltham, MA). Aliquots of total homogenates containing 30 μg protein were denatured with Laemmli buffer, separated by reducing 10% polyacrylamide gel electrophoresis, and electroblotted onto PVDF membranes. Membranes were blocked for 1 h in 5% (w/v) defatted milk and subsequently incubated in the presence of the corresponding primary antibody (1:1,000 dilution) overnight at 4 °C. After incubation for 90 min at room temperature in the presence of the corresponding secondary antibody (HRP conjugated) (1:10,000 dilution), the conjugates were visualized uding an ECL system in a Phosphoimager 840 (Amersham Pharmacia Biotech. Inc., Piscataway, NJ).

2.7. Immunohistochemistry

Immunohistochemistry (IHC) of ileum samples was done as previously described [10]. Tissues were fixed in 4% (w/v) solution of paraformaldehyde in PBS overnight, rinsed with PBS and stored in 70% (v/v) ethanol. Samples were embedded in paraffin and 5 μm sections were obtained. Once deparaffinized, sections were processed for antigen retrieval by incubation in 10 mM sodium citrate buffer (pH 6.0) containing 0.05% (v/v) Tween 20 at 95 °C for 10 min, washed twice with 0.1% (v/v) Triton X-100 in PBS, blocked for 45 min in 2% (v/v) donkey serum in 0.1% (v/v) Triton X-100 in M PBS, and incubated overnight at 4 °C with primary antibody for MUC2 (1:200). Sections were washed in PBS and incubated for 2 h at room temperature with Cy3-conjugated donkey anti-mouse or anti-rabbit IgG (1:500) (Jackson ImmunoResearch Co. Laboratories West Grove, PA). After immunostaining, cell nuclei were stained with 1 μg/ml Hoechst 33342 and sections were imaged using an Olympus FV 1000 laser scanning confocal microscope (Olympus, Japan). Olympus Fluoview version 4.0 software was used to merge images. Four slices per animal and four animals from each group were analyzed.

2.8. Microbiota analysis

Cecum content samples were collected in sterile tubes for subsequent investigation of the microbiome through high throughput sequencing. Samples were stored at −80 °C until processing for DNA extraction. Genomic DNA was extracted from cecal samples using the Zymo Research Fecal DNA Miniprep Kit per the manufacturer's instructions (Zymo Research, Irvine, CA, USA). The V4 region of the 16S rRNA gene was amplified by targeted barcoded primers F515 (5′-*NNN NNNNN*GTGTGCCAGCMGCCGCGGTAA-3′) and R806 (5′-GGACTACH-VGGGTWTCTAAT-3′) as previously described [20]. Amplicons were then pooled and purified with the QIAquick PCR Purification Kit (Qiagen, Germantown, MD, USA) and taken to the UC Davis Genome Center DNA Technologies Sequencing Core for library preparation and paired-end sequenced on an Illumina Miseq. PEAR [21] was used to merge the paired end reads and they were subsequently demultiplexed using the FASTX Toolkit (http://hannonlab.cshl.edu/fastx_toolkit/). Cutadapt was then used to trim off barcodes and primers from reads [22]. Read quality filtering, OTU picking using the implemented swarm method, filtering the OTU table, rarefaction, and beta diversity data analysis was carried out within the QIIME software package (University of Colorado, Boulder, CO, USA. version 1.9.1) [23]. Swarm was used within the QIIME package as the operational taxonomic unit clustering method [24]. Beta diversity metrics were calculated based on Unifrac distances. Results were visualized by nonmetric multidimensional scaling (NMDS) as implemented in the vegan package in R.

3. Statistical analysis

Data were analyzed by one-way analysis of variance (ANOVA) using Statview 5.0 (SAS Institute Inc., Cary, NC). Fisher least significance difference test was used to examine differences between group means. A p value < 0.05 was considered statistically significant. Data are shown as mean ± SE.

4. Results

4.1. Supplementation with AC improved HFD-associated increased intestinal permeability and endotoxemia

As previously described [17], consumption of the HFD for 14 weeks resulted in obesity and insulin resistance in C57BL/6J mice, which were mitigated by AC supplementation. Although no significant changes were observed in the small intestine length and weight (data not shown); the colon weight and the colon weight/length ratio were higher in HF compared to C and CA mice (Fig. 1A). AC supplementation mitigated the increased colon weight/length ratio associated with HFD consumption.

Intestinal permeability was evaluated by measuring the paracellular transport of FITC-dextran after 8 weeks on the corresponding diets. FITC-dextran transport was five times higher in mice consuming the HFD compared to controls, but this higher level was not observed in the HFA group (Fig. 1B). An increase in intestinal permeability can lead to the paracellular transport of luminal endotoxins into the circulation. In agreement with FITC-dextran results, plasma endotoxin levels were 98% higher in HF compared to C and CA mice (Fig. 1C). In mice fed the HFD and supplemented with AC, plasma endotoxin concentrations were similar to control values.

4.2. AC prevented TNFα-induced permeabilization of Caco-2 cell monolayers

We next investigated if the AC mix fed to mice could also inhibit *in vitro* the permeabilization of Caco-2 cell monolayers. Permeabilization was induced by exposure to a pro-inflammatory challenge (TNFα) and was evaluated by measuring the paracellular transport of FITC-dextran and the monolayer TEER. Incubation in the presence of TNFα in the lower chamber (basolateral side) caused a 1.1-fold increase in FITC-dextran paracellular transport and a 32% decrease in TEER (Fig. 2A and
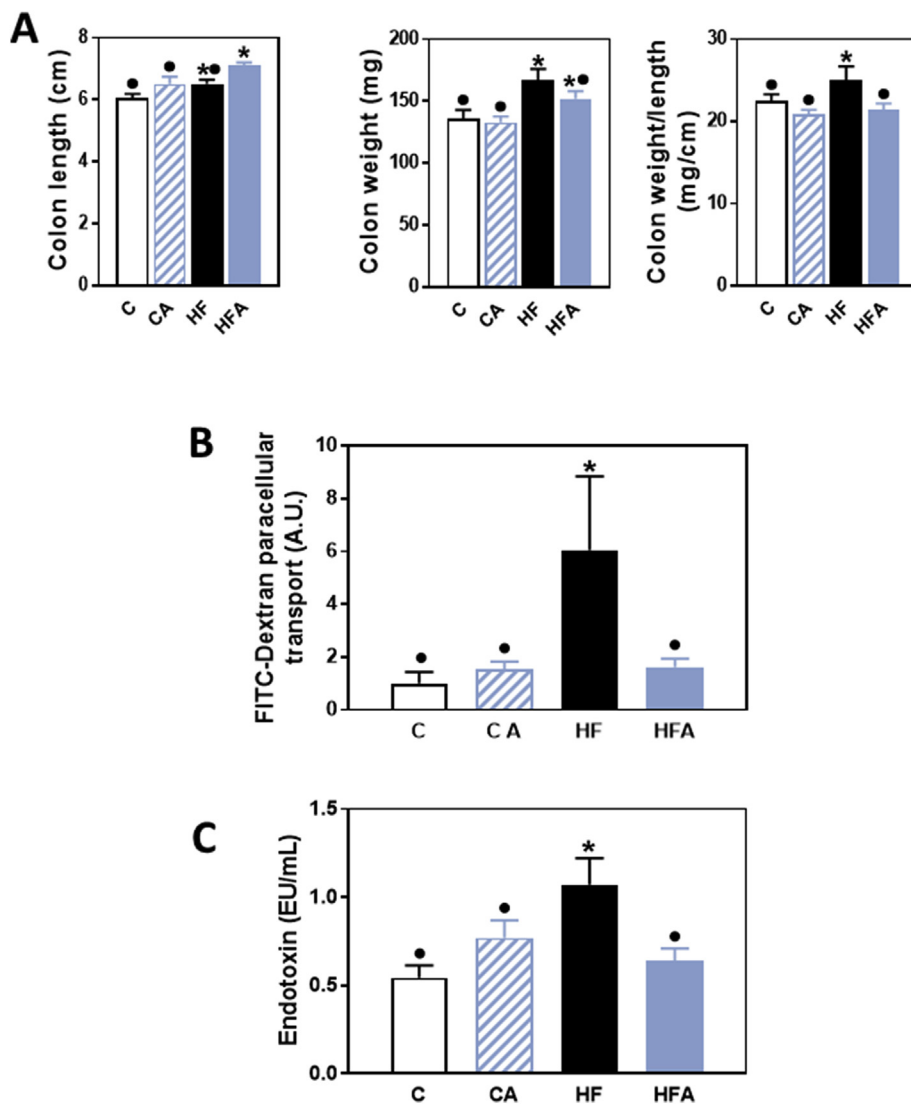
Fig. 1. Effects of AC supplementation on HFD-mediated changes on colon weight and length, and intestinal permeability in mice. Mice were fed a control diet (empty bars), the control diet supplemented with 40 mg AC/kg body weight (dashed bars), a HFD (black bars), or the HFD supplemented with 40 mg AC /kg body weight (blue bars) for 14 weeks. **A**- Colon weight, length and weight/length ratio. **B,C**- Intestinal permeability was evaluated by measuring at week 8 on the diets, FITC-dextran permeability **(B)**, and at week 14, plasma endotoxin **(C)**. Results are shown as means ± SE and are the average of 9–10 animals/group. Values having different superscripts are significantly different (p < 0.05, One-way ANOVA test). (For interpretation of the references to colour in this figure legend, the reader is referred to the Web version of this article.)

B). Addition of the AC mix to the upper chamber (apical side) fully prevented the increase in FITC-dextran permeability at both, 2.5 and 5 μg AC mix/ml, and the decrease in TEER at the highest AC mix concentration tested (5 μg AC/ml).

We subsequently tested the capacity of individual AC and PCA at approximately the concentrations present in 5 μg mix/ml (1 μM cyanidin, 0.5 μM delphinidin, 0.1 μM peonidin, and 0.5 μM PCA) to prevent TNFα-induced Caco-2 monolayer permeabilization. PCA and the 3-O-glucosides of cyanidin and delphinidin, but not peonidin, inhibited the paracellular transport of FITC-dextran (Fig. 2C) and the decrease in TEER (Fig. 2D) promoted by TNFα.

4.3. AC prevented HFD-mediated alterations in TJ protein expression and modulated GLP-2

As previously observed [10], consumption of the HFD for 14 weeks was associated with an altered expression of TJ proteins in the ileum. In HF mice, a 50, 73 and 44% decrease in ileum occludin, ZO-1 and claudin-1 protein levels was observed compared to controls as measured by Western blot. Supplementation of HFD-fed mice with AC either partially (ZO-1) or fully (occludin and claudin-1) inhibited HFD-mediated decreases in TJ protein expression (Fig. 3 A).

GLP-2 is an intestinal hormone that has important trophic and TJ protective functions at the intestinal epithelium. Mice supplemented

with AC showed a significant increase in plasma GLP-2 levels compared to control and HF mice. In AC40 and HFA40 mice plasma GLP-2 concentrations were 2- and 1.4-fold higher than in non-supplemented controls (Fig. 3B).

4.4. AC modulated signaling pathways and redox-related events that affect TJ structure and function

Both the NF-κB and ERK1/2 pathways are involved in the modulation of TJ structure and function. To evaluate the activation of these cascades we measured the phosphorylation of p65 (NF-κB) and ERK1/2 by Western blot. p65 and ERK1/2 phosphorylation levels were 54 and 47% higher in HF mouse ileum compared to controls (Fig. 4A). Downstream, ileum myosin light chain (MLC) phosphorylation levels were 60% higher in the HF than in controls. Supplementation with AC prevented HFD-associated increases in p65, ERK1/2 and MLC phosphorylation (Fig. 4A).

Given that the upregulation of NADPH oxidases NOX1 and NOX4 and oxidative stress are observed in association with intestinal permeabilization in HFD-fed mice [9], we next investigated the capacity of AC supplementation to mitigate NADPH oxidases and inducible nitric oxide synthase (NOS2) upregulation, and the occurrence of ileum oxidative damage by measuring 4-HNE-protein adducts. NOX1, NOX4 and NOS2 protein levels were higher in HF ileum (60, 40 and 81%,
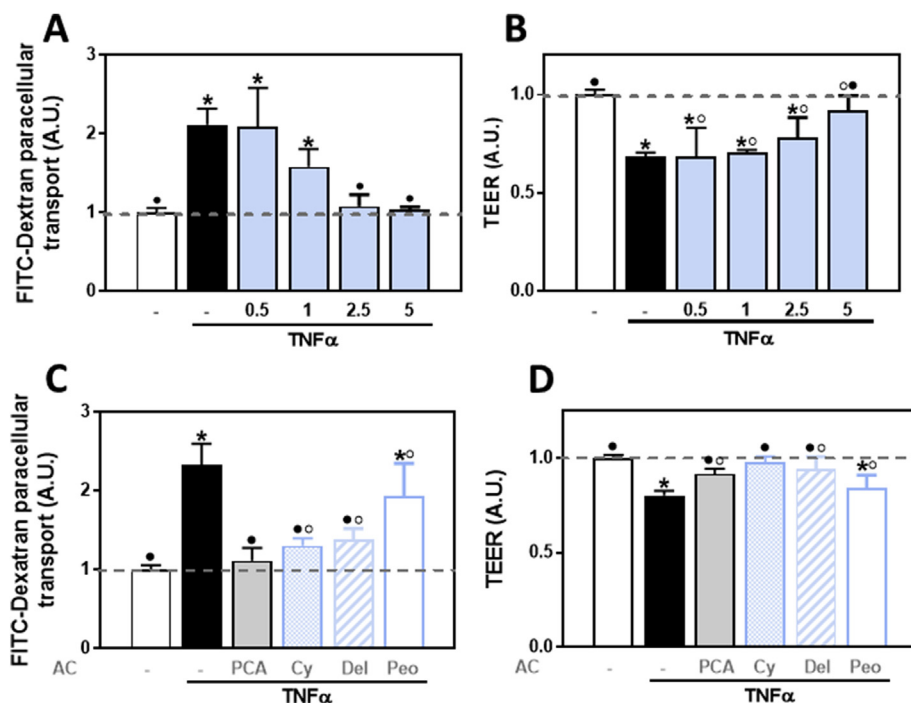
Fig. 2. Effects of the AC-rich mix, PCA, and 3-O-glucosides of cyanidin, delphinidin, and peonidin on TNFα-induced permeabilization of Caco-2 cell monolayers. Caco-2 cell monolayers were pre-incubated for 24 h with IFNγ (10 ng/ml) to upregulate the TNFα receptor. Then, the following compounds were added to the upper chamber and cells incubated for 30 min: **A,B-** 0.5–5 μg AC mix/ml or **C,D-** the concentration of the individual components present in the mix at a 5 μg AC/ml concentration: 0.5 μM PCA, 1 μM cyanidin-3-O-glucoside, 0.5 μM delphinidin-3-O-glucoside, or 0.1 μM peonidin. TNFα (5 ng/ml) was subsequently added to the lower chamber and cells incubated for further 6 h. Caco-2 cell monolayer permeability was evaluated by measuring **(A,C)** FITC-dextran paracellular transport (FITC-Dextran) and **(B,D)** TEER. Basal TEER values were 350–420 $\Omega\,cm^2$ and basal average FITC-dextran clearance value was 65 nl. $h^{-1}.cm^{-2}$. Results are shown as mean ± SE of 4–6 independent experiments. Results (A.U.: arbitrary units) were normalized to control values (1, dashed line). Values having different superscripts are significantly different ($p < 0.05$, One-way ANOVA).

respectively) than in controls and HFA mice (Fig. 4B). This was associated with a 40% increase in 4-HNE-protein adducts corresponding to the 40 kDa protein band. AC supplementation mitigated HFD-triggered NADPH oxidases (NOX1 and NOX4) and NOS2 upregulation, and the increased 4-HNE-protein adducts levels.

4.5. Effects of cyanidin, delphinidin, peonidin and PCA on TNFα-induced NF-κB and ERK1/2 activation, NADPH oxidase upregulation, and oxidative stress in Caco-2 cells

NF-κB and ERK signaling pathways are activated downstream of TNFα binding to its receptor and are major players in TNFα-induced permeabilization of the intestinal barrier. In Caco-2 cells, exposure to TNFα increased the phosphorylation of NF-κB (p65), ERK 1/2 (49 and 160%, respectively), and MLC (59%), compared to controls (Fig. 5A). At the tested concentrations, PCA, cyanidin-3-O-glucoside and the AC mix, fully prevented p65, ERK1/2, and MLC phosphorylation. Delphinidin-3-O-glucoside inhibited TNFα-triggered p65 phosphorylation, and peonidin3-O-glucoside had no effect on these parameters. On the other hand, PCA, cyanidin, peonidin and the AC mix inhibited TNFα-mediated NOX1 and NOX4 upregulation, and prevented 4-HNE-protein adduct formation, a marker of protein/lipid oxidation (Fig. 5B).
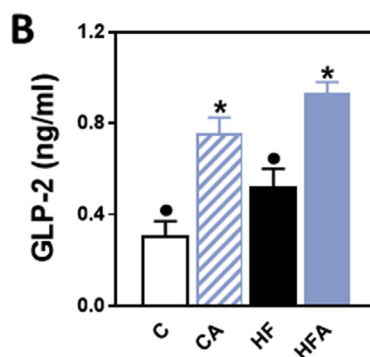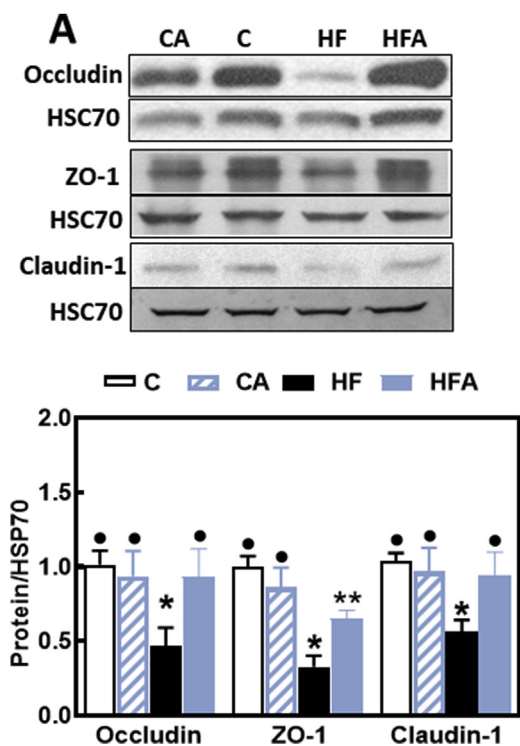

Fig. 3. AC mitigates HFD-mediated decrease in TJ protein expression and modulates hormones that regulate TJ structure and function. Mice were fed a control diet (empty bars), the control diet supplemented with 40 mg AC/kg body weight (dashed bars), a HFD (black bars), or the HFD supplemented with 40 mg AC /kg body weight (blue bars) for 14 weeks. **A-** Ileum protein levels of occludin, ZO-1 and claudin-1 were measured by Western blot. Bands were quantified and values normalized to HSC70 levels (loading control). Values were referred to those of the control group (empty bars). **B-** Plasma GLP-2 concentrations were measured by ELISA. Results are shown as mean ± SE of 6–8 animals/treatment. Values having different superscripts are significantly different ($p < 0.05$, One-way ANOVA test). (For interpretation of the references to colour in this figure legend, the reader is referred to the Web version of this article.)

Fig. 4. Effects of AC on signaling molecules that regulate TJ structure and function, on the upregulation of ileum NADPH oxidases and NOS2, and on protein oxidation induced by HFD consumption in mice. A- Phosphorylation levels of p65 (Ser536), ERK1/2 (Thr202/Tyr204) and MLC (Ser19) in total ileum homogenates were measured by Western blot. Bands were quantified and values normalized to non-phosphorylated protein levels. B- Total protein levels of NOX1, NOX4, NOS2 and 4-HNE-protein adducts (MW: 40 kDa). Proteins were measured by Western blot in the ileum of mice fed a control diet (empty bars), the control diet supplemented with 40 mg AC/kg body weight (dashed bars), a HFD (black bars), or the HFD supplemented with 40 mg AC /kg body weight (blue bars) for 14 weeks. Bands were quantified and values normalized to HSC70 levels (loading control). Results were referred to those of the control group (C). Results are shown as mean ± SE of 6–8 animals/treatment. Values having different superscripts are significantly different (p < 0.05, One-way ANOVA test). (For interpretation of the references to colour in this figure legend, the reader is referred to the Web version of this article.)
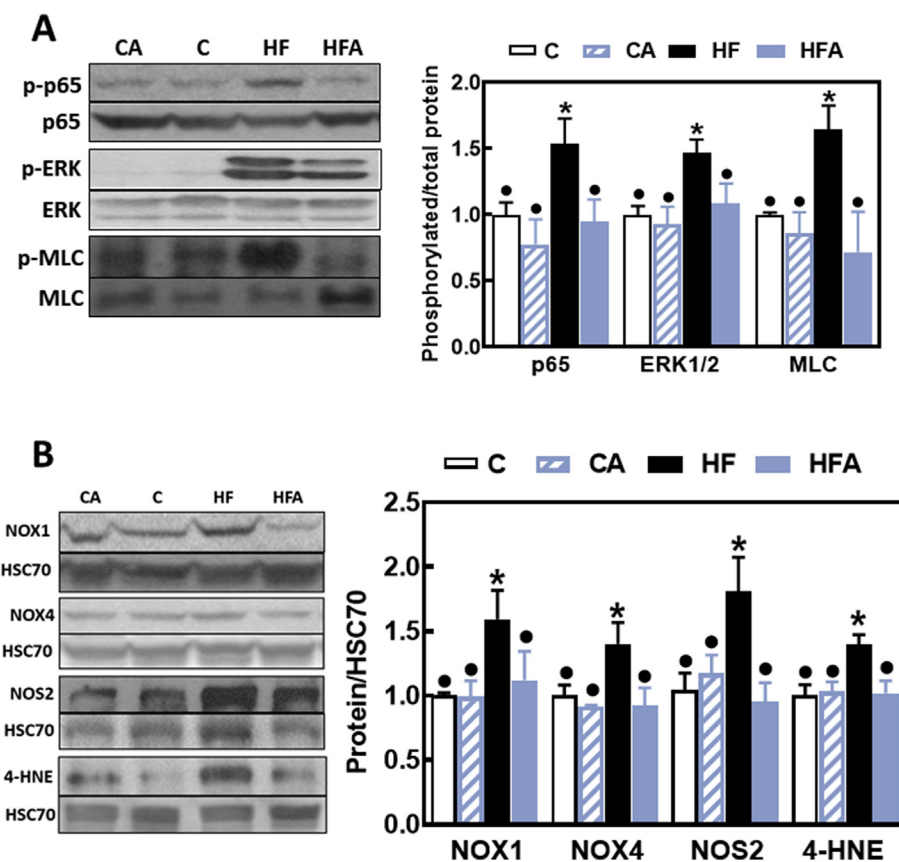

Fig. 5. Effects of AC on TNFα-induced upregulation of signals that regulate TJ structure and the associated upregulation of NADPH oxidases and protein/ lipid oxidation in Caco-2 cells. Caco-2 cells were incubated for 6 h at 37 °C in the absence of additions (control, C) (empty bars); or after addition of 5 ng/ml TNFα in the absence (TNFα) (black bars) or the presence of 0.5 μM PCA (grey bars); 1 μM cyanidin-3-O-glucoside (dotted bars), 0.5 μM delphinidin-3-O-glucoside (dashed bars), 0.1 μM peonidin (white bars) or 5 μg AC/ml (light blue bars). A- Phosphorylation levels of p65 (Ser536), ERK1/2 (Thr202/Tyr204), and MLC (Ser19), and B- total protein levels of NOX1, NOX4, and 4-HNE-protein adducts (MW: 40 kDa) were measured by Western blot. Bands were quantified and values normalized to (A) the non-phosphorylated protein and B- β-actin levels. Results were referred to control group values (C). Results are shown as mean ± SE of 6 independent experiments. Values having different superscripts are significantly different (p < 0.05, One-way ANOVA test). (For interpretation of the references to colour in this figure legend, the reader is referred to the Web version of this article.)
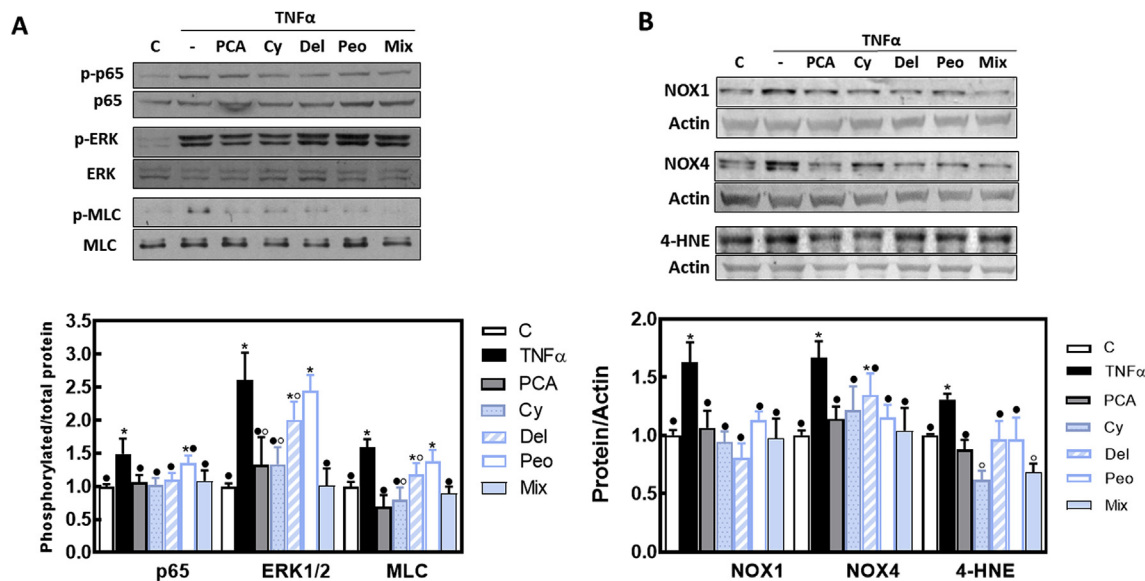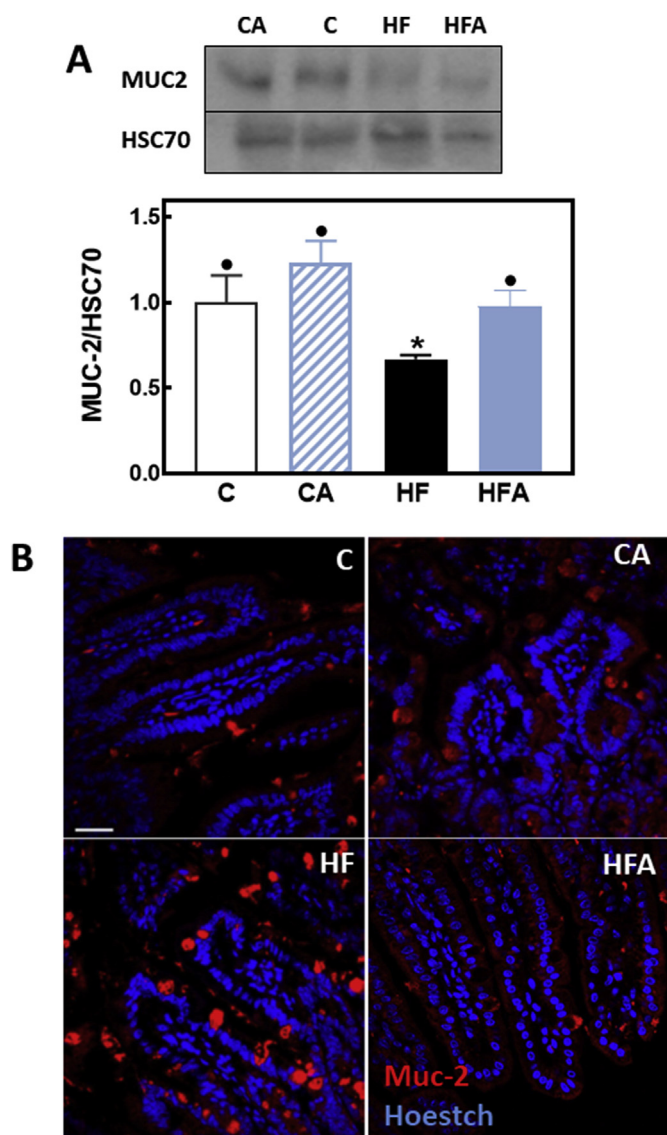
Fig. 6. AC mitigates HFD-mediated alterations in MUC2 levels and distribution in mouse ileum. Mice were fed a control diet (empty bars), the control diet supplemented with 40 mg AC/kg body weight (dashed bars), a HFD (black bars), or the HFD supplemented with 40 mg AC /kg body weight (blue bars) for 14 weeks. **A-** The ileum content of MUC2 was measured by Western blot. Bands were quantified and values referred to HSC70 levels (loading control). Results were referred to those of the control group (C). Results are shown as mean ± SE of 6–8 animals/treatment. Values having different superscripts are significantly different (p < 0.05, One-way ANOVA test). **B-** Representative images for immunohistochemistry and confocal microscopy for MUC2 (red fluorescence). Nuclei were stained with Hoechst (blue fluorescence) (Bar: 50 μm). (For interpretation of the references to colour in this figure legend, the reader is referred to the Web version of this article.)

Interestingly, the AC mix and cyanidin-3-O-glucoside decreased the levels of 4-HNE-protein adducts at lower levels than those of control (no TNFα added) cells.

4.6. AC prevented the adverse effects of HFD consumption on MUC2 secretion from goblet cells

MUC2 is a major component of the mucus layer that protects the intestinal epithelium monolayer and constitutes the first line of immunological defense [25]. We next measured the amount and distribution of MUC2 in mouse ileum. MUC2 protein levels measured by
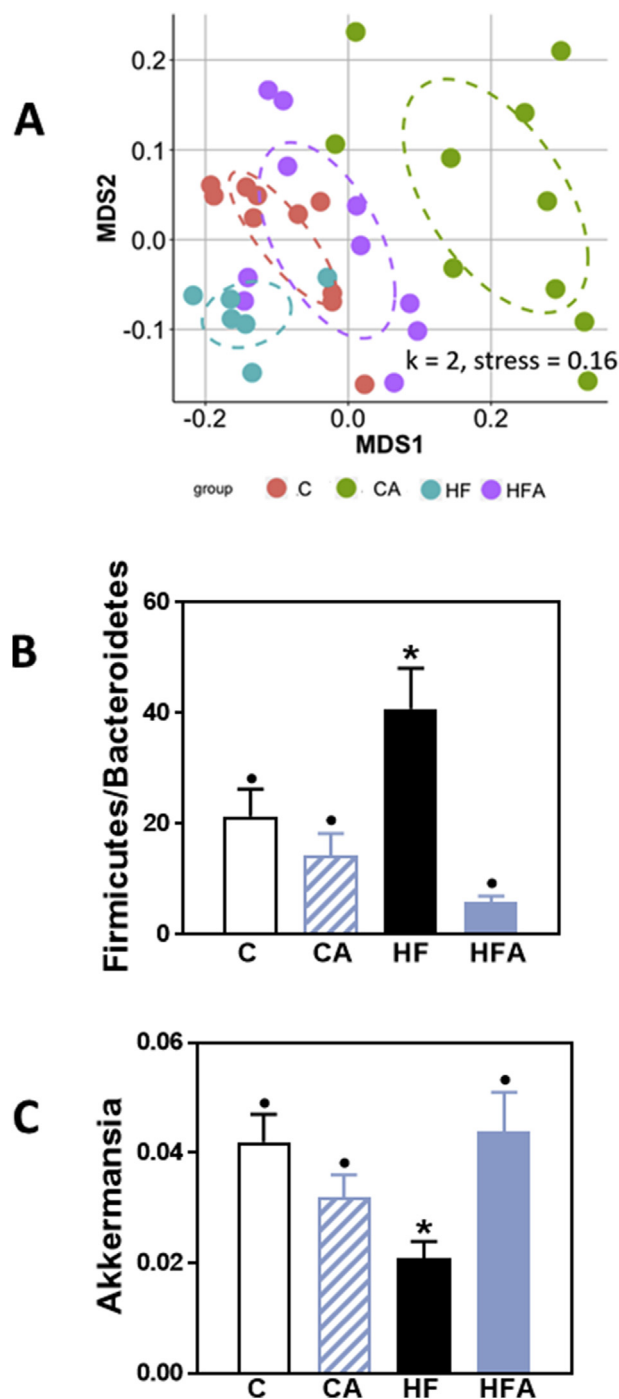

Fig. 7. AC prevents HFD-induced alterations in mouse cecal microbiota. Mice were fed a control diet (red dots, empty bars), the control diet supplemented with 40 mg AC/kg body weight (green dots, dashed bars), a HFD (blue dots, black bars), or the HFD supplemented with 40 mg AC /kg body weight (violet dots, blue bars) for 8 weeks. **A-** Changes in cecum microbiota were assessed by clustering of samples based on diet. NMDS was performed based on the weighted UniFrac distance matrix generated from sequencing fecal 16S rRNA gene The X-axis represents the tertiary coordinate, the Y-axis represents the secondary coordinate. Axis numbering represents the relative distance between samples based on the weighted UniFrac distance matrix. **B-** Ratio of fecal *Firmicutes/Bacteroidetes* abundance, and **C-** fecal *Akkermansia* relative abundance. **B,C-** Results are shown as mean ± SE of 6–10 animals/treatment. Values having different superscripts are significantly different (p < 0.05, One-way ANOVA test). (For interpretation of the references to colour in this figure legend, the reader is referred to the Web version of this article.)

Western blot were 33% lower in HF than in control and HFA mice (Fig. 6A). IHC characterization of MUC2 distribution showed that consumption of the HFD caused the accumulation of MUC2 in Goblet cells, which was prevented by AC supplementation (Fig. 6B)

4.7. AC affects the composition of the microbiota both in control- and HFD-fed mice

Long-term consumption of a HFD affects the composition of the microbiota. Overall evaluation of cecal microbiota profiles was done by nonmetric multidimensional scaling (NMDS). After 8 weeks on the corresponding diets, the microbiota of HF mice clustered separately from that of control mice (Fig. 7 A), while HFD-fed mice supplemented with AC showed a clustering similar to that of controls. Interestingly, the fecal microbiota from mice fed the control diet supplemented with AC showed a clear cluster separation compared to unsupplemented controls.

Among the microbiota changes associated with HFD consumption, we found the widely described increase in the ratio *Firmicutes/Bacteroidetes* (Fig. 7B), and also a 50% decrease in *Akkermansia* relative abundance (Fig. 7C). AC supplementation prevented both the altered *Firmicutes/Bacteroidetes* ratio and the decrease in *Akkermansia* relative abundance.

5. Discussion

Chronic consumption of a HFD by C57BL/6J mice caused intestinal permeabilization, endotoxemia, and dysbiosis, which were prevented by AC dietary supplementation. AC modulated key events that regulate epithelial cell monolayer permeability and endotoxemia, i.e. NADPH oxidase upregulation, oxidative stress, NF-κB and ERK1/2 activation, and downstream MLC phosphorylation. Furthermore, AC supplementation was associated with increased plasma GLP-2 concentrations, and mitigation of HFD-mediated impaired MUC2 secretion and dysbiosis. The above AC beneficial effects can all contribute to the protection of intestinal barrier function, prevention of endotoxemia and enhancement of metabolic control.

The present work is an extension of a previous study in which, using the same set of mice, we observed that AC (cyanidin and delphinidin) supplementation, mitigates the development of insulin resistance, liver inflammation and steatosis in mice fed a high fat diet [17]. Mechanistically, these AC-mediated protective actions were associated with the inhibition of upregulation of NADPH oxidases, oxidative stress, and activation of redox-sensitive signaling (JNK, NF-κB) in liver and adipose tissue [17]. In the current study, we observed that the AC supplementation prevented HFD-mediated intestinal permeabilization and endotoxemia, which can both explain findings of local (ileal NF-κB activation and NOS2 upregulation) and systemic inflammation [17]. In agreement with previous findings, both *in vivo* and *in vitro*, the AC mix and the major individual components, i.e. cyanidin, delphinidin and PCA, but not peonidin, protected Caco-2 cell monolayers from TNFα-induced permeabilization [16]. Stressing the physiological relevance of these findings, the concentrations of AC affording full protection against TNFα-induced Caco-2 monolayer permeabilization are more than 10 times lower than those found in human ileum after consumption of 300 g of raspberries [26]. Intestinal permeabilization allows the passage into the circulation of pro-inflammatory bacterial components, including endotoxins. This is proposed to underlie in part obesity- and Western style diet-associated pathologies, including T2D and NAFLD [2,5,27–29]. Thus, mitigation of intestinal permeabilization may contribute to the beneficial actions of AC on diet-induced obesity, insulin resistance, and steatosis.

The intestinal epithelium is a single cell layer composed of different cell types with multiple functions, forming a barrier between the external environment and the body [7]. Monolayer permeabilization can be due to HFD and/or inflammation-induced alterations in expression of specific TJ components which are determinants of the functionality of the intestinal barrier. In this regard, both dietary fat and the associated increase in bile acid production contribute to suppression of TJ protein expression (claudin-1, claudin-3, occludin and junctional adhesion molecule-1) and to intestinal permeabilization in rats [30]. We observed that the chronic consumption of a HFD decreased the expression of ZO-1, occludin and claudin-1 in the ileum of C57BL/6J mice. These alterations were partially or completely prevented by AC, providing a mechanism to in part explain AC capacity to prevent intestinal permeabilization and endotoxemia *in vivo*. These effects of AC were similar to those observed in mice fed a HFD and supplemented with the flavanol (−)-epicatechin [10]. It is important to consider that the chemical structure of cyanidin, delphinidin, PCA, and (−)-epicatechin includes a free 3′-hydroxyl group in the B ring that is methylated in peonidin. Therefore, it can be speculated that the bioactivity of certain ACs and flavanols may rely on the catechol structure of the B-ring.

NF-κB and ERK1/2 are activated by oxidative stress [31–33] and it has been reported previously that H_2O_2 moderately activates ERK1/2 in Caco-2 cells [34] and causes MDCK cell monolayer permeabilization in a ZO-1 and ERK1/2-dependent manner [35]. In addition, H_2O_2 activates NF-κB in Caco-2 cells leading to an increased expression of NOS2, and oxidation/nitration of cytoskeletal proteins [36]. Compounds, i.e. (−)-epicatechin and apocynin, that inhibit the superoxide/H_2O_2-generating NADPH oxidase activity/expression and prevent protein/lipid oxidation, were able to concurrently mitigate TNFα-induced Caco-2 cell monolayer permeabilization [10,37] and HFD-induced intestinal permeabilization and endotoxemia in mice [10]. In the present study, we observed that AC supplementation prevented the upregulation of NOX1 and NOX4 expression and the associated increase in oxidative damage (actin-4-HNE adducts) in the ileum of mice fed a HFD. Similar effects were observed for the mix and for individual AC and PCA in Caco-2 monolayers treated with TNFα. Both NOX1 and NOX4 expression are in part regulated by NF-κB, with several κB sites present in the promoter region of both genes [38]. Stressing the association of oxidant production with NF-κB activation, the regulation of NOS2 followed the same pattern as that of NOX1 and NOX4. Thus, our results support the concept that the prevention of NOX4 and NOX1 upregulation of increased superoxide/H_2O_2 production and activation of NF-κB and ERK1/2 are relevant mechanisms involved in the protection of the intestinal barrier by AC. Additionally, it should be mentioned that 4-HNE per se can participate in the development of intestinal chronic inflammation contributing to permeabilization and carcinogenesis, particularly in the context of high fat consumption [39].

Obesity and consumption of high fat diets have a major influence on intestinal microbiota diversity, representation of bacterial genes and bacteria composition [40,41], which can result not only in alterations in proper intestinal function, but in systemic consequences affecting the physiology of other organs. Chronic HFD consumption is associated with an increased relative abundance of *Firmicutes* and a decrease of *Bacteroidetes* and *Akkermansia* [40–42]. Accordingly, we observed an increased *Firmicutes/Bacteroidetes* relative abundance ratio and an altered clustering of the microbiota in HFD-fed mice. These changes were not observed in HFD-fed mice supplemented with AC. It should be pointed out that there is limited conclusive evidence as to the mechanisms explaining how these changes in microbiota are molecularly associated with optimal physiology. In this paper we investigated two determinants of intestinal health which are known to be in part modulated by the microbiota composition, i.e. plasma GLP-2 and ileum mucus levels.

The HFD did not impact GLP-2-plasma concentrations. However, AC supplementation to mice fed either the control diet or the HFD caused an increase in GLP-2 plasma concentrations. Although such increases could be triggered through other mechanisms, it is well accepted that the microbiota have a role influencing the release of glucagon-like peptides, i.e. GLP-1 and GLP-2, by L enteroendocrine cells [43]. This is

highly relevant to AC-mediated improvement of HFD-induced insulin resistance and steatosis not only given the intestinal barrier trophic and protective actions of GLP-2 [44], but also to its capacity to decrease hepatic lipid deposition and modulate energy homeostasis [45,46].

A mucus layer covers the intestinal epithelium constituting the first barrier against harmful bacteria, toxins, proteolytic enzymes, and other substances present in the lumen [47]. This layer is composed of highly glycosylated proteins, MUC2 being the most abundant. MUC2, as well as other mucins, are synthesized and released by Goblet cells. Even a short-term exposure to a high fat diet causes an altered release of MUC2 and its accumulation inside Goblet cells [40]. We observed in the ileum from HFD-fed mice, the accumulation of MUC2 fluorescence in Goblet cells and a decreased overall amount of MUC2. Supplementation with AC prevented cell accumulation of MUC2, and mitigated the HFD-mediated decrease in MUC2 ileal content. Among the factors regulating MUC2 synthesis, Akkermansia intestinal abundance is associated with increased MUC2 production [48]. Thus, the observed prevention by AC of HFD-mediated decrease of Akkermasia relative abundance may in part explain AC's capacity to mitigate the ileum MUC2 decrease in HFD-fed mice.

The inhibition of redox-sensitive signals involved in TJ dynamics/ structure modulation and the downregulation of enzymes generating superoxide/H_2O_2 (NOX1/NOX4) and nitric oxide (iNOS) appear to be relevant to AC capacity to preserve barrier integrity. The conservation of an appropriate intestinal microbiota composition and function can also contribute to the observed benefits. Thus, the capacity of AC, particularly delphinidin and cyanidin, and its metabolite PCA, to preserve GI physiology, is not only relevant locally, but can also contribute to their capacity to mitigate pathologies, i.e. insulin resistance and steatosis, triggered by high fat consumption [17].

Conflicts of interest

Acknowledgements

References

[1] J.R. Turner, Intestinal mucosal barrier function in health and disease, Nat. Rev. Immunol. 9 (11) (2009) 799–809.

[2] M.K. Piya, A.L. Harte, P.G. McTernan, Metabolic endotoxaemia: is it more than just a gut feeling? Curr. Opin. Lipidol. 24 (1) (2013) 78–85.

[3] F. de Faria Ghetti, D.G. Oliveira, J.M. de Oliveira, L. de Castro Ferreira, D.E. Cesar, A.P.B. Moreira, Influence of gut microbiota on the development and progression of nonalcoholic steatohepatitis, Eur. J. Nutr. 57 (3) (2018) 861–876.

[4] H. Tilg, A. Kaser, Gut microbiome, obesity, and metabolic dysfunction, J. Clin. Investig. 121 (6) (2011) 2126–2132.

[5] P.D. Cani, J. Amar, M.A. Iglesias, M. Poggi, C. Knauf, D. Bastelica, A.M. Neyrinck, F. Fava, K.M. Tuohy, C. Chabo, A. Waget, E. Delmee, B. Cousin, T. Sulpice, B. Chamontin, J. Ferrieres, J.F. Tanti, G.R. Gibson, L. Casteilla, N.M. Delzenne, M.C. Alessi, R. Burcelin, Metabolic endotoxemia initiates obesity and insulin resistance, Diabetes 56 (7) (2007) 1761–1772.

[6] F. Laugerette, M. Alligier, J.P. Bastard, J. Drai, E. Chanseaume, S. Lambert-Porcheron, M. Laville, B. Morio, H. Vidal, M.C. Michalski, Overfeeding increases postprandial endotoxemia in men: inflammatory outcome may depend on LPS transporters LBP and sCD14, Mol. Nutr. Food Res. 58 (7) (2014) 1513–1518.

[7] M.A. Odenwald, J.R. Turner, The intestinal epithelial barrier: a therapeutic target? Nat. Rev. Gastroenterol. Hepatol. 14 (1) (2017) 9–21.

[8] P.D. Cani, R. Bibiloni, C. Knauf, A. Waget, A.M. Neyrinck, N.M. Delzenne, R. Burcelin, Changes in gut microbiota control metabolic endotoxemia-induced

[9] inflammation in high-fat diet-induced obesity and diabetes in mice, Diabetes 57 (6) (2008) 1470–1481.

[9] Z.Y. Kho, S.K. Lal, The human gut microbiome - a potential controller of wellness and disease, Front. Microbiol. 9 (2018) 1835.

[10] E. Cremonini, Z. Wang, A. Bettaieb, A.M. Adamo, E. Daveri, D.A. Mills, K.M. Kalanetra, F.G. Haj, S. Karakas, P.I. Oteiza, (-)-Epicatechin protects the intestinal barrier from high fat diet-induced permeabilization: implications for steatosis and insulin resistance, Redox Biol 14 (2018) 588–599.

[11] A.P. Moreira, T.F. Texeira, A.B. Ferreira, C. Peluzio Mdo, C. Alfenas Rde, Influence of a high-fat diet on gut microbiota, intestinal permeability and metabolic endotoxaemia, Br. J. Nutr. 108 (5) (2012) 801–809.

[12] P.D. Cani, S. Possemiers, T. Van de Wiele, Y. Guiot, A. Everard, O. Rottier, L. Geurts, D. Naslain, A. Neyrinck, D.M. Lambert, G.G. Muccioli, N.M. Delzenne, Changes in gut microbiota control inflammation in obese mice through a mechanism involving GLP-2-driven improvement of gut permeability, Gut 58 (8) (2009) 1091–1103.

[13] L.V. Hooper, D.R. Littman, A.J. Macpherson, Interactions between the microbiota and the immune system, Science 336 (6086) (2012) 1268–1273.

[14] C.L. Maynard, C.O. Elson, R.D. Hatton, C.T. Weaver, Reciprocal interactions of the intestinal microbiota and immune system, Nature 489 (7415) (2012) 231–241.

[15] P.I. Oteiza, C.G. Fraga, D.A. Mills, D.H. Taft, Flavonoids and the gastrointestinal tract: local and systemic effects, Mol. Asp. Med. 61 (2018) 41–49.

[16] E. Cremonini, A. Mastaloudis, S.N. Hester, S.V. Verstraeten, M. Anderson, S.M. Wood, A.L. Waterhouse, C.G. Fraga, P.I. Oteiza, Anthocyanins inhibit tumor necrosis alpha-induced loss of Caco-2 cell barrier integrity, Food Funct 8 (8) (2017) 2915–2923.

[17] E. Daveri, E. Cremonini, A. Mastaloudis, S.N. Hester, S.M. Wood, A.L. Waterhouse, M. Anderson, C.G. Fraga, P.I. Oteiza, Cyanidin and delphinidin modulate inflammation and altered redox signaling improving insulin resistance in high fat-fed mice, Redox Biol 18 (2018) 16–24.

[18] S. Reagan-Shaw, M. Nihal, N. Ahmad, Dose translation from animal to human studies revisited, FASEB J. 22 (3) (2008) 659–661.

[19] A. Fischer, M. Gluth, U.F. Pape, B. Wiedenmann, F. Theuring, D.C. Baumgart, Adalimumab prevents barrier dysfunction and antagonizes distinct effects of TNF-alpha on tight junction proteins and signaling pathways in intestinal epithelial cells, Am. J. Physiol. Gastrointest. Liver Physiol. 304 (11) (2013) G970–G979.

[20] S.A. Frese, K. Parker, C.C. Calvert, D.A. Mills, Diet shapes the gut microbiome of pigs during nursing and weaning, Microbiome 3 (2015) 28.

[21] J. Zhang, K. Kobert, T. Flouri, A. Stamatakis, PEAR: a fast and accurate Illumina Paired-End reAd mergeR, Bioinformatics 30 (5) (2014) 614–620.

[22] M. Martin, Cutadapt removes adapter sequences from high-throughput sequencing reads, EMBnet.journal 17 (2011) 10–12.

[23] J.G. Caporaso, C.L. Lauber, W.A. Walters, D. Berg-Lyons, C.A. Lozupone, P.J. Turnbaugh, N. Fierer, R. Knight, Global patterns of 16S rRNA diversity at a depth of millions of sequences per sample, Proc. Natl. Acad. Sci. U. S. A. 108 (Suppl 1) (2011) 4516–4522.

[24] F. Mahe, T. Rognes, C. Quince, C. de Vargas, M. Dunthorn, Swarm: robust and fast clustering method for amplicon-based studies, PeerJ 2 (2014) e593.

[25] M.E. Johansson, G.C. Hansson, Immunological aspects of intestinal mucus and mucins, Nat. Rev. Immunol. 16 (10) (2016) 639–649.

[26] R. Gonzalez-Barrio, G. Borges, W. Mullen, A. Crozier, Bioavailability of anthocyanins and ellagitannins following consumption of raspberries by healthy humans and subjects with an ileostomy, J. Agric. Food Chem. 58 (7) (2010) 3933–3939.

[27] A.L. Harte, M.C. Varma, G. Tripathi, K.C. McGee, N.M. Al-Daghri, O.S. Al-Attas, S. Sabico, J.P. O'Hare, A. Ceriello, P. Saravanan, S. Kumar, P.G. McTernan, High fat intake leads to acute postprandial exposure to circulating endotoxin in type 2 diabetic subjects, Diabetes Care 35 (2) (2012) 375–382.

[28] L. Valentini, S. Ramminger, V. Haas, E. Postrach, M. Werich, A. Fischer, M. Koller, A. Swidsinski, S. Bereswill, H. Lochs, J.D. Schulzke, Small intestinal permeability in older adults, Phys. Rep. 2 (4) (2014) e00281.

[29] C.A. Thaiss, M. Levy, I. Grosheva, D. Zheng, E. Soffer, E. Blacher, S. Braverman, A.C. Tengeler, O. Barak, M. Elazar, R. Ben-Zeev, D. Lehavi-Regev, M.N. Katz, M. Pevsner-Fischer, A. Gertler, Z. Halpern, A. Harmelin, S. Aamar, P. Serradas, A. Grosfeld, H. Shapiro, B. Geiger, E. Elinav, Hyperglycemia drives intestinal barrier dysfunction and risk for enteric infection, Science 359 (6382) (2018) 1376–1383.

[30] T. Suzuki, H. Hara, Dietary fat and bile juice, but not obesity, are responsible for the increase in small intestinal permeability induced through the suppression of tight junction protein expression in LETO and OLETF rats, Nutr Metab (Lond) 7 (2010) 19.

[31] H. Sies, C. Berndt, D.P. Jones, Oxidative stress, Annu. Rev. Biochem. 86 (2017) 715–748.

[32] S.E. Oh, M.M. Mouradian, Cytoprotective mechanisms of DJ-1 against oxidative stress through modulating ERK1/2 and ASK1 signal transduction, Redox Biol 14 (2018) 211–217.

[33] C. Ott, K. Jacobs, E. Haucke, A. Navarrete Santos, T. Grune, A. Simm, Role of advanced glycation end products in cellular signaling, Redox Biol 2 (2014) 411–429.

[34] S. Basuroy, P. Sheth, D. Kuppuswamy, S. Balasubramanian, R.M. Ray, R.K. Rao, Expression of kinase-inactive c-Src delays oxidative stress-induced disassembly and accelerates calcium-mediated reassembly of tight junctions in the Caco-2 cell monolayer, J. Biol. Chem. 278 (14) (2003) 11916–11924.

[35] S. Bilal, S. Jaggi, D. Janosevic, N. Shah, S. Teymour, A. Voronina, J. Watari, J. Axis, K. Amsler, ZO-1 protein is required for hydrogen peroxide to increase MDCK cell paracellular permeability in an ERK 1/2-dependent manner, Am. J. Physiol. Cell Physiol. 315 (3) (2018) C422–C431.

[36] A. Banan, L.J. Zhang, M. Shaikh, J.Z. Fields, A. Farhadi, A. Keshavarzian, Novel effect of NF-kappaB activation: carbonylation and nitration injury to cytoskeleton and disruption of monolayer barrier in intestinal epithelium, Am. J. Physiol. Cell

Physiol. 287 (4) (2004) C1139–C1151.

[37] T.C. Contreras, E. Ricciardi, E. Cremonini, P.I. Oteiza, (-)-Epicatechin in the pre-vention of tumor necrosis alpha-induced loss of Caco-2 cell barrier integrity, Arch. Biochem. Biophys. 573 (2015) 84–91.

[38] A. Manea, L.I. Tanase, M. Raicu, M. Simionescu, Transcriptional regulation of NADPH oxidase isoforms, Nox1 and Nox4, by nuclear factor-kappaB in human aortic smooth muscle cells, Biochem. Biophys. Res. Commun. 396 (4) (2010) 901–907.

[39] D. Rossin, S. Calfapietra, B. Sottero, G. Poli, F. Biasi, HNE and cholesterol oxidation products in colorectal inflammation and carcinogenesis, Free Radic. Biol. Med. 111 (2017) 186–195.

[40] J. Tomas, C. Mulet, A. Saffarian, J.B. Cavin, R. Ducroc, B. Regnault, C. Kun Tan, K. Duszka, R. Burcelin, W. Wahli, P.J. Sansonetti, T. Pedron, High-fat diet modifies the PPAR-gamma pathway leading to disruption of microbial and physiological ecosystem in murine small intestine, Proc. Natl. Acad. Sci. U. S. A. 113 (2016) E5934–E5943.

[41] P.J. Turnbaugh, M. Hamady, T. Yatsunenko, B.L. Cantarel, A. Duncan, R.E. Ley, M.L. Sogin, W.J. Jones, B.A. Roe, J.P. Affourtit, M. Egholm, B. Henrissat, A.C. Heath, R. Knight, J.I. Gordon, A core gut microbiome in obese and lean twins, Nature 457 (7228) (2009) 480–484.

[42] P.D. Cani, A.M. Neyrinck, F. Fava, C. Knauf, R.G. Burcelin, K.M. Tuohy,

G.R. Gibson, N.M. Delzenne, Selective increases of bifidobacteria in gut microflora improve high-fat-diet-induced diabetes in mice through a mechanism associated with endotoxaemia, Diabetologia 50 (11) (2007) 2374–2383.

[43] P.D. Cani, A. Everard, T. Duparc, Gut microbiota, enteroendocrine functions and metabolism, Curr. Opin. Pharmacol. 13 (6) (2013) 935–940.

[44] P.E. Dube, P.L. Brubaker, Frontiers in glucagon-like peptide-2: multiple actions, multiple mediators, Am. J. Physiol. Endocrinol. Metab. 293 (2) (2007) E460–E465.

[45] S. Baldassano, A. Amato, G.F. Caldara, F. Mule, Glucagon-like peptide-2 treatment improves glucose dysmetabolism in mice fed a high-fat diet, Endocrine 54 (3) (2016) 648–656.

[46] S. Baldassano, A. Amato, F. Mule, Influence of glucagon-like peptide 2 on energy homeostasis, Peptides 86 (2016) 1–5.

[47] T. Pelaseyed, J.H. Bergstrom, J.K. Gustafsson, A. Ermund, G.M. Birchenough, A. Schutte, S. van der Post, F. Svensson, A.M. Rodriguez-Pineiro, E.E. Nystrom, C. Wising, M.E. Johansson, G.C. Hansson, The mucus and mucins of the goblet cells and enterocytes provide the first defense line of the gastrointestinal tract and in-teract with the immune system, Immunol. Rev. 260 (1) (2014) 8–20.

[48] A. Everard, C. Belzer, L. Geurts, J.P. Ouwerkerk, C. Druart, L.B. Bindels, Y. Guiot, M. Derrien, G.G. Muccioli, N.M. Delzenne, W.M. de Vos, P.D. Cani, Cross-talk be-tween Akkermansia muciniphila and intestinal epithelium controls diet-induced obesity, Proc. Natl. Acad. Sci. U. S. A. 110 (22) (2013) 9066–9071.